Investigation of the Effect of Deformable Trailing Edge Geometry Control Systems on Flutter Velocity

Mac Gaunaa
Risø National Laboratory, Wind Energy Department,
Building VEA-118, B.O. Box 49, Frederiksborgvej 399, DK-4000 Roskilde
Email: mac.gaunaa@risoe.dk

Abstract

Recent simulations in 2D and 3D as well as wind tunnel testing has shown a big potential for fatigue load reduction using Deformable Trailing Edge Geometry (DTEG). The present work continues the investigations by determining the effect of the DTEG control system on flutter velocity in the 2D case. The focus of this work is on the difference in flutter velocity without flaps, using conventional rigid flaps and continuously DTEG. The effect of the flap control system parameters, including both PD control parameters as well as control system timelag is investigated.

Keywords: aeroservoelasticity**,** stability, control.

1 Introduction

The development in wind turbines has led to relatively softer blades over the years. This makes fast regulation using the pitch system unpractical or even impossible since the blades are considerably deflected in the flapwise direction at most wind speeds. Recent work has shown a big potential of fatigue load reduction using Deformable Trailing Edge Geometry (DTEG), where local variations in geometry, and hence aeroelastic control along the blade, is possible. DTEG can be considered a generalization of the commonly used rigid flaps (as found on conventional aeroplanes), where the deformation of the trailing edge is described by a mode shape. The mode shape for conventional rigid flaps is linear. Deformation modes that are not linear can be obtained using for instance piezoelectric actuators. Figure 1 show an example of a DTEG.

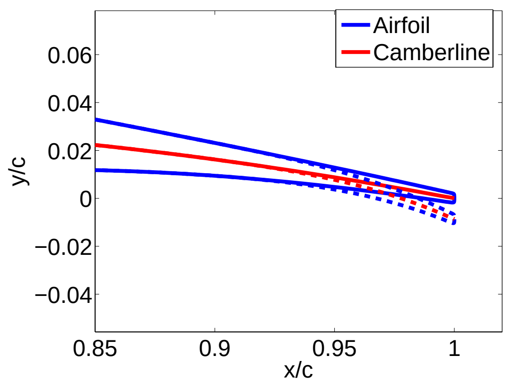

Figure 1: Example of a 10% chord-length DTEG deflected 5 degrees. Note that the deflection mode shape is not linear as opposed to conventional trailing edge flaps.

The work carried out on using DTEG for fatigue load reduction so far has analysed the load reduction potential using 2D [1] and 3D [2] simulations, which has revealed a big potential for fatigue load reduction using this type of control surfaces. Futhermore, a 2D airfoil section equipped with piezoelectric actuators have been tested in the Velux wind tunnel [3] to validate the aerodynamic model used in the simulations.

Much work has been carried out on load reduction using the pitch systems on the wind turbines [4, 5]. Regarding the stability of wind turbine wings, Lobitz [6] concluded that the classical flutter limit is reached for a typical 1.5 MW blade if the rotational velocity is multiplied by a factor two. However, Hansen [7] concluded that single blade analysis does generally not yield conservative estimation of the onset of instabilities.

The present work continues the investigations of DTEG by determining the effect of DTEG on flutter velocity in the 2D case. Specifically, focus will be on the difference in flutter velocity without flaps, using conventional rigid flaps and continuously DTEG. Moreover, the effect of the flap control system will be investigated.

The equations that describe the 2D aeroservoelastic system are rewritten in their equivalent state space formulation. Therefore, the response of the linear system is describable by a matrix equation, for which stability is determined using an eigenvalue approach. The aerodynamic model used was developed by Gaunaa [8], and is a potential-flow model that can predict the response of arbitrarily deforming thin airfoils for non-stalling flows, which correspond to the outer section son a PRVS wind turbine. The structural model is a linear spring/damper system for the elastic deformation of a rigid airfoil to which the inertial forces associated with deflection of the trailing edge are added. The last part of the aeroservoelastic system is the control part, for which a PD regulator on the flapwise position is used. Furthermore, system time-delay in the control system is modelled using a first-order differential equation.

The present work is part of the ADAPWING2 project carried out at Risø.

2 Theoretical Model

The full aeroservoelastic model consists of models for aerodynamics, elastic deformation of the whole airfoil section in the heave and torsional directions, and a model for the control system including control system time lag. The submodels are described briefly below.

2.1 Aerodynamics

The aerodynamic model used in the present work was developed by Gaunaa [8], and is a generalization of the work by Theodorsen [9] to take into account the unsteady aerodynamic forces from an arbitrary deformation of the camberline. If the airfoil can move in the heave-direction, Y, (perpendicular to the wind) and in the torsional direction, α, and the deformation of the aifoil trailing edge is given by the trailing edge angle, β, as defined on Figure 2, then the unsteady aerodynamic forces (Lift and Moment) can be expressed as

$$\underline{F}_{Aero} = \underline{f}_{A1}(\alpha,\dot{\alpha},\ddot{\alpha},\dot{Y},\ddot{Y},\beta,\dot{\beta},\ddot{\beta}) + \underline{f}_{A2}(\underline{z}_A).$$

The functions $\underline{f}_{A1}$ and $\underline{f}_{A2}$ are linear, and $\underline{z}_A$ is the state variables describing the time lag linked to the development of the unsteady wake. These are determined from the first order differential equation

$$\dot{z}_{Ai} + b_i \tfrac{2}{c} V z_{Ai} = b_i A_i \tfrac{2}{c} VQ$$

Q is given by

$$Q = \alpha_{3/4} - f_{A3}(\beta,\dot{\beta}),$$

where $\alpha_{3/4}$ is the relative three quarter angle of attack at the three quarter chord point, and f_{A3} is a linear function. The remaining constants in the differential equation are the constants that describe the approximation of the step response function. The values of these are given in Table 1.

i	A_i	b_i
1	0.0821	0.0199
2	0.1429	0.7817
3	0.3939	0.1453

Table 1: Constants for the step response function, $\Phi(\tau) = 1 - \sum_i A_i e^{-b_i \tau}$, for the Risø-B1-18 airfoil.

A thorough description of the aerodynamic model can be found in [8].

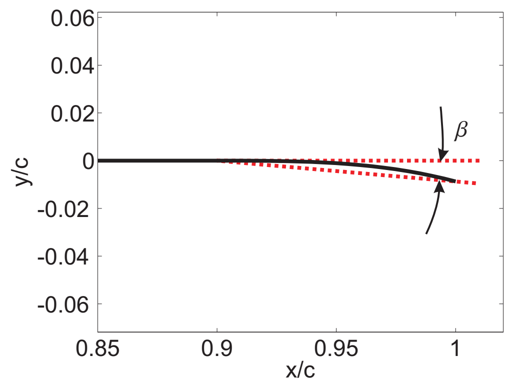

Figure 2: Definition of the trailing edge deformation angle β, which in the shown case is 5 degrees. The shown deflection shape is the curved one used in the computations to follow.

2.2 Heaving Motion

The force balance between elastic, damping, aerodynamic and intertial forces in the heaving direction is given by the second order differential equation

$$\ddot{Y}M + Ml\ddot{\alpha} + \dot{Y}C_Y + YK_Y = L_{Aero} + L_{Fict}$$

L_{Aero} is the lift forces from the aerodynamic model, and L_{Fict} is the addition to the inertial lift forces from acceleration of the trailing edge.

$$L_{Fict} = -\ddot{\beta}\int_{xLe}^{xTe} \rho_s(x) y_\beta(x) dx$$

$\rho_s(x)$ and $y_\beta(x)$ are the unit depth density and trailing edge unit deformation shape functions, respectively. *x* is the local chordwise coordinate.

2.3 Pitching Motion

Analogous to the Equation for the heaving motion, the second order Equation for the torsional motion reads

$$\ddot{\alpha}(I_{CG} + Ml^2) + Ml\ddot{Y} + \alpha C_\alpha + (\alpha - \alpha_K)K = M_{Aero} + M_{Fict}$$

M_{Aero} is the moment from the aerodynamic forces, and M_{Fict} is the addition to the intertial moment from the inertial forces due to the acceleration of the trailing edge.

$$M_{Fict} = x_a L_{Fict} + \ddot{\beta}\int_{xLe}^{xTe} x\rho_s(x) y_\beta(x) dx$$

2.4 Control Algorithm

In the earlier works regarding fluctuating load alleviation using DTEG [1,2] it was concluded, that a simple Proportional Differential (PD) control on the heave coordinate Y was quite effective in terms of reducing flapwise fatigue loads. Therefore a simple PD control algorithm is studied in this work also:

$$\beta_{Ctrl} = (Y - Y_I)A_Y + \dot{Y}B_Y .$$

Y_I is the running mean heave coordinate $Y_I = \frac{1}{\Delta T}\int_{t-\Delta T}^{t} Y(\tau)d\tau$

2.5 Time-lag model

The time-lag in the control system is modelled with a first-order differential equation

$$\dot{\beta} + b_{Lag}\beta = b_{Lag}\beta_{Ctrl}$$

where $b_{Lag} = -\ln(1/2)/t_{1/2}$.

This way the time lag is quantified with the control system half-time $t_{1/2}$. This time is the time it takes for the physical trailing edge angle, β, to reach half the value of a step signal in the control algorithm output, β_{Ctrl}.

2.4 Stability

If oscillations around a mean value is considered, then all sub-models described above can be combined into one single matrix equation

$\underline{\underline{\tilde{A}}}\dot{\underline{x}} + \underline{\underline{\tilde{B}}}\underline{x} = \underline{0}$, where

$\underline{x} = \left[z_{A1}, z_{A2}, z_{A3}, \beta, \alpha, \dot{\alpha}, Y, \dot{Y}\right]^T$.

The stability of such a matrix system can be determined from standard eigenvalue tools. The one used in the present work is from Matlab's standard built-in functions.

3 Basic Computational Case

The positioning of the mass, elastic and aerodynamic centers in the aerofoil design is an important consideration in any discussion of aeroelastic stability; especially for the occurrence of flutter. For the specific blade section used in the present investigations, the aerodynamic and structural properties are given in Table 2 below. The values are identical to the one used by Buhl [1].

Description	unit	value
Chord-length	m	1.0
Position of elastic axis from LE	m	0.3
Position of CG from LE	m	0.35
Total mass of airfoil per unit depth	kg	40
Intertial moment around CG		2.0
Eigen-freq. in heave direction	Hz	1.0
Eigen-freq. in pitching direction	Hz	10.0
Linear damping in the heave direction		0
Linear damping in the pitching direction		0
Proportional Control Constant		-400
Differential Control Constant		-25
Control time lag reaction half-time, $t_{1/2}$	s	0.0
Air density	Kg/m^3	1.225

Table 2: Structural data for the 2D profile section.

Furthermore, the mass distribution, $\rho_s(x)$, for determining the intertial loads from deflection of the Trailing edge of the airfoil is shown in Figure 3 below.

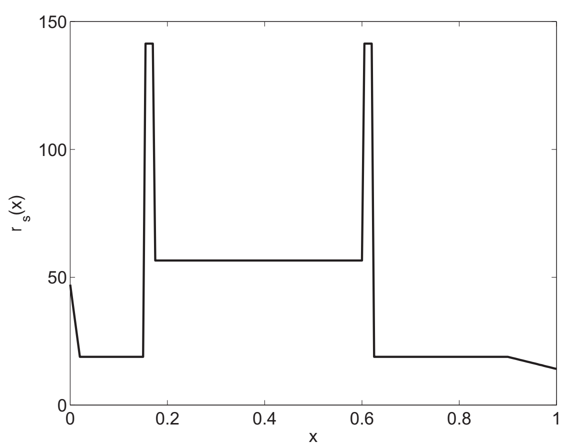

Figure 3: Mass distribution, $\rho_s(x)$, for the basic computational case.

According to Buhl [1], the reduction of the standard deviation of the normal force with the basic control settings as shown in Table 2 yields a 74% reduction compared to the uncontrolled case.

4 Verification and Results

The model is verified against the time-marching DTEG time simulation tool used by Buhl [1]. The flutter speeds, ie. the speeds at which initial amplitudes increase (negative total damping), were within a few percent of the ones found with the time stepping method for the test cases investigated. However, a more rigorous validation of the code with the time-stepping method could be justified.

For referene, the flutter speeds without control, and with the basic control algorithm using both a flat and a curved flap without time-lag was computed. The results are shown in Table 3.

Computational case	Basic comp. case. No flap/control	Basic comp. case. Flat flap	Basic comp. case. Curved flap
Flutter velocity	142.9 m/s	95.8 m/s	90.7 m/s

Table 3: Flutter velocities for the basic computational case with no flap/no control, with a flat falp and with a curved flap.

As seen from the results in Table 3, the addition of a trailing edge flap control system with the chosen control algorithm lowers the flutter velocity considerably, for both flap deformation mode shapes.

Figure 4 below shows the influence of the trailing edge flap mass on the stability limits.

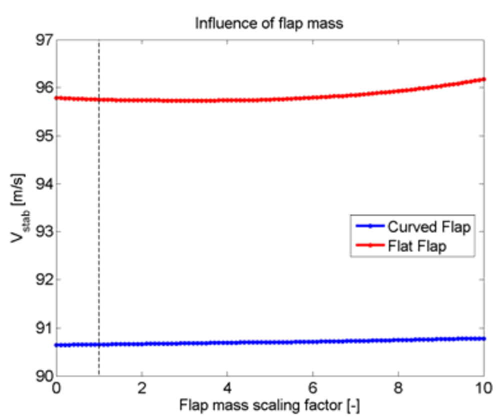

Figure 4: Influence of the mass of the flap on the flutter velocity in the case of a curved and a flat flap. When the flap mass scaling factor is unity, we have the basic computational case.

As seen from Figure 4, there is almost no influence from the flap mass on the flutter velocity. This may be attributed to the relatively weak coupling between the driven trailing edge flap with it's associated mass, and the heave and pitching force balances. The intertial forces fed into the heave and pitching equations are small compared to the other terms: heave/pitch coupling and aerodynamic forces.

An investigation of the effect of the control constants A_Y and B_Y on the flutter velocity is shown in Figure 5.

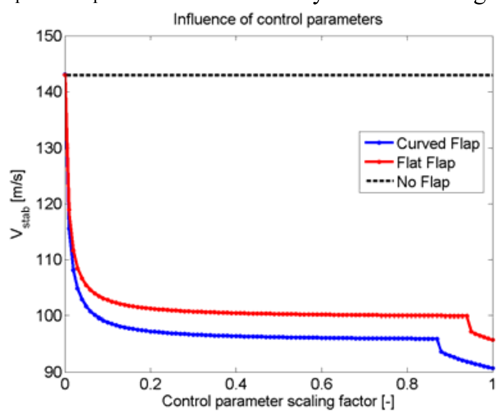

Figure 5: Influence of the control algorithm parameters on the flutter velocity. No time-lag is present in the control system. When the control parameter scaling factor factor is one, the basic computational case is obtained.

The basic computational control system constants are both multiplied with the scaling factor, shown along the x-axis of Figure 5. The results indicate that the flutter velocity drops very rapidly from having no control to just controlling slightly (control parameter scaling facor = 0.1) , after which the flutter velocity remains fairly constant up to control scaling parameter 0.9 in the curved flap case and 0.95 in the flat flap case, after which it drops slightly.

In the investigations on the load reduction potential of trailing edge flap control methods it was concluded that system time lag was a major factor in the potential. In order to investigate the effect of time lag on the flutter velocity, Figure 6 show the influence of system reaction half-time on the flutter velocity.

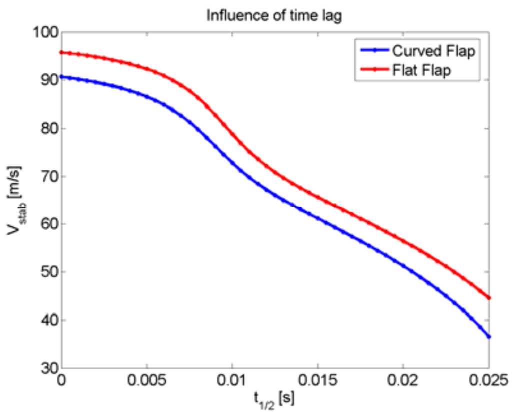

Figure 6: Influence of the control system time lag on flutter velocity. When $t_{1/2}$ is zero, we have the basic computational case.

From the figures, it is seen that the effect of the time-lag on the flutter velocity is negative. An increased time-lag results in a reduced flutter velocity.

As c concluding remark in the results section, it should be mentioned that these computations are all based on the same basic computational case, and that most of these conclusions may have had different conclusions if the basic computational case had been different. This is among the further work to be done with the current analysis tool.

5 Conclusions

A new model for determination of the stability of the equilibrium of the 2D aeroservoelastic has been proposed. A preliminary verification against a time-stepping method show good agreement. The model was used to investigate the effect of the DTEG control system on the stability of the equilibrium of a 2D wind turbine section. The results indicate that the relative air velocity at which instabilities occur may be reduced significantly with the addition of DTEG control systems, and that the type of deformation shape was of minor importance. However, further studies are needed to investigate fully the implications of adding a DTEG control system on the stability limits of the equilibrium state of the 2D system.

Acknowledgement

The author gratefully acknowledges that this work was partially funded by the Danish Research Council.

References

[1].Buhl, T., Gaunaa, M., Bak, C.; "Potential load reduction using airfoils with variable trailing edge geometry", J. Solar Energy Engineering. November 2005. pp 503-516.

[2].Andersen, P.B.; "Load alleviation on wind turbines using variable airfoil geometry", Masters Thesis, Technical University of Denmark.

[3].Buhl, T., Gaunaa, M., Bak, C., Andersen, P.B. "Load Alleviation Using Variable Trailing Edge Geometry", Windstat, To appear.

[4]. Larsen, T., Madsen. H., and Thomsen, K. "Active Load Reduction Using Individual Pitch, Based on Local Flow Measurements", Proc. EWEA, The Science of Making Torque From Wind. April 2004. Netherlands

[5]. Bossanyi, E. "Developments in Individual Pitch Control" Proc. EWEA, The Science of Making Torque From Wind. April 2004. Netherlands

[6]. Lobitz D.W., "Aeroelastic stability predictions for a MW-sized blade", Wind Energy, Vol. 7(3), pp. 211-224, 2004.

[7].Hansen M.H., "Aeroelastic Stability Analysis of Wind Turbines Using an Eigenvalue Approach". Wind Energy, 2003; 7: 133–143.

[8].Gaunaa, M.; "Unsteady potential-flow forces on a thin variable geometry airfoil undergoing arbitrary motion", Risø-R-1478(EN), To appear.

[9].Theodorsen, T.; "General Theory of Aerodynamical Instability and the Mechanism of Flutter". NACA Report 496. 1935.